

Pressure-induced phase transition in transition metal trifluorides

Peng Liu(刘鹏), Meiling Xu(徐美玲), Jian Lv(吕健), Pengyue Gao(高朋越), Chengxi Huang(黄呈熙),Yinwei Li(李印威), Jianyun Wang(王建云), Yanchao Wang(王彦超), and Mi Zhou(周密)
Citation: Chin. Phys. B, 2022, 31 (**10**): 106104. DOI: 10.1088/1674-1056/ac5887
Journal homepage: http://cpb.iphy.ac.cn; http://iopscience.iop.org/cpb

What follows is a list of articles you may be interested in

Onion-structured transition metal dichalcogenide nanoparticles by laser fabrication in liquids and atmospheres

Le Zhou(周乐), Hongwen Zhang(张洪文), Qian Zhao(赵倩), and Weiping Cai(蔡伟平)
Chin. Phys. B, 2022, 31 (**7**): 076106. DOI: 10.1088/1674-1056/ac539c

Effect of structural vacancies on lattice vibration, mechanical, electronic, and thermodynamic properties of Cr_5BSi_3

Tian-Hui Dong(董天慧), Xu-Dong Zhang(张旭东), Lin-Mei Yang(杨林梅), and Feng Wang(王峰)
Chin. Phys. B, 2022, 31 (**2**): 026101. DOI: 10.1088/1674-1056/ac11e2

Prediction of scandium tetraboride from first-principles calculations: Crystal structures, phase stability, mechanical properties,and hardness

Bin-Hua Chu(初斌华) and Yuan Zhao(赵元)
Chin. Phys. B, 2021, 30 (**7**): 076107. DOI: 10.1088/1674-1056/abe116

Effects of 3d-transition metal doping on the electronic and magnetic properties of one-dimensional diamond nanothread

Zhenzhen Miao(苗珍珍), Can Cao(曹粲), Bei Zhang(张蓓), Haiming Duan(段海明), Mengqiu Long(龙孟秋)
Chin. Phys. B, 2020, 29 (**6**): 066101. DOI: 10.1088/1674-1056/ab84dd

Geoscience material structures prediction via CALYPSO methodology

Andreas Hermann
Chin. Phys. B, 2019, 28 (**10**): 106107. DOI: 10.1088/1674-1056/ab43bc

---

SPECIAL TOPIC — Celebrating the 70th Anniversary of the Physics of Jilin University

Pressure-induced phase transition in transition metal trifluorides

Peng Liu(刘鹏)[1,†], Meiling Xu(徐美玲)[2,†], Jian Lv(吕健)[1], Pengyue Gao(高朋越)[1], Chengxi Huang(黄呈熙)[3], Yinwei Li(李印威)[2], Jianyun Wang(王建云)[1,‡], Yanchao Wang(王彦超)[1], and Mi Zhou(周密)[1,§]

[1] *State Key Laboratory of Superhard Materials & International Center for Computational Method and Software, College of Physics, Jilin University, Changchun* 130012, *China*

[2] *Laboratory of Quantum Functional Materials Design and Application, School of Physics and Electronic Engineering, Jiangsu Normal University, Xuzhou* 221116, *China*

[3] *MIIT Key Laboratory of Semiconductor Microstructure and Quantum Sensing, Nanjing University of Science and Technology, Nanjing* 210094, *China*

(Received 24 January 2022; revised manuscript received 15 February 2022; accepted manuscript online 25 February 2022)

As a fundamental thermodynamic variable, pressure can alter the bonding patterns and drive phase transitions leading to the creation of new high-pressure phases with exotic properties that are inaccessible at ambient pressure. Using the swarm intelligence structural prediction method, the phase transition of TiF_3, from *R*–3*c* to the *Pnma* phase, was predicted at high pressure, accompanied by the destruction of TiF_6 octahedra and formation of TiF_8 square antiprismatic units. The *Pnma* phase of TiF_3, formed using the laser-heated diamond-anvil-cell technique was confirmed via high-pressure x-ray diffraction experiments. Furthermore, the *in situ* electrical measurements indicate that the newly found *Pnma* phase has a semiconducting character, which is also consistent with the electronic band structure calculations. Finally, it was shown that this pressure-induced phase transition is a general phenomenon in ScF_3, VF_3, CrF_3, and MnF_3, offering valuable insights into the high-pressure phases of transition metal trifluorides.

Keywords: high-pressure structure transition, crystal structure prediction, high-pressure x-ray diffraction experiments, transition metal

PACS: 61.50.Ks, 64.70.K–, 62.50.–p

DOI: 10.1088/1674-1056/ac5887

1. Introduction

Transition metal trifluorides, a class of materials with the chemical formula MF_3 (M = Sc, Ti, V, Cr, Mn, and so forth) have attracted considerable attentions owing to their versatile applications in negative thermal expansion materials,[1–4] batteries,[5–7] and hydrogen storage materials.[8–12] More importantly, they have been demonstrated to be ideal materials to study the Jahn–Teller and spin–orbit coupling effects.[13,14] Under ambient conditions, MF_3 usually adopts a simple perovskite-like structure with a completely vacant A site,[15–19] in which the metal atom is surrounded by a tilted octahedron of corner-shared fluorine atoms. Moreover, the tilting angle of the octahedron decreases with increasing temperature, causing a high-temperature phase transition to the cubic ReO_3-type structure.[17,20] It is essential to note that the physical and chemical properties of MF_3 are generally associated with structural parameters, such as polyhedral volume and octahedral tilt.[21–28] Therefore, investigating the structural changes in MF_3 will provide new insights for designing functional materials.

It is well known that pressure is a key thermodynamic variable that modifies the crystal structure and effectively controls material properties. For example, high-pressure experiments have led to the discovery of novel materials with unique properties (e.g., high-temperature superconductors such as H_3S,[29,30] LaH_{10},[31,32] and C–S–H[33]). The high pressure thus offers exciting opportunities for discovering new materials that do not exist under ambient conditions.[34–40] High-pressure does not necessitate the destruction of the MF_6 octahedron in MF_3 systems. In practice, the pressure-induced structural evolution is only the cooperative tilting of the MF_6 octahedra,[41–43] which can be summarized as follows: (i) an elongation of the MF_6 octahedra along the *c* axis leads to a small octahedral strain, (ii) the MF_6 octahedral strain disappears, and (iii) MF_6 octahedral elongation occurs along the *a* axis.

In this work, we adopted a combination of first-principle calculations and experiments to explore the high-pressure phase of TiF_3. Our results suggest that TiF_3 transforms from the rhombohedral (*R*–3*c*) phase to an orthorhombic (*Pnma*) phase at high pressure, accompanied by the destruction of the TiF_6 octahedra and formation of TiF_8 square antiprismatic units. The high-pressure *Pnma* phase of TiF_3 is confirmed by the laser-heated diamond-anvil-cell experiment and shows semiconducting character with a band gap of 2.65 eV. We fur-

[†]These authors contributed equally to this work.

[‡]Corresponding author. E-mail: wangjianyun@jlu.edu.cn

[§]Corresponding author. E-mail: mzhou@jlu.edu.cn

© 2022 Chinese Physical Society and IOP Publishing Ltd

ther confirmed that the pressure-induced transition from *R*–3*c* to *Pnma* phase is a general trend in transition metal trifluorides, such as ScF_3, VF_3, CrF_3, and MnF_3.

2. Methods

***Ab initio* calculations** The search for TiF_3 structures (1–4 formula units) was performed at pressures of 20 GPa and 50 GPa via an unbiased swarm intelligence based method, Crystal structure AnaLYsis by Particle Swarm Optimization (CALYPSO),[44–46] which is designed to search for the most stable or metastable structures of given compounds.[47–57] Our first-principle calculations were based on density functional theory,[58] as implemented in the VASP package.[59] The core electrons were treated by the projector-augmented wave approximation,[60] and the exchange–correlation functional was given by the generalized gradient approximation parameterized by Perdew, Burke, and Ernzerhof.[61] The plane-wave cutoff energy was set to 800 eV, and Monkhorst–Pack *k* meshes with a spacing of $2\pi \times 0.03$ Å^{-1} were chosen for Brillouin zone sampling to ensure that all the energy calculations converged well to ~ 1 meV/atom. The Heyd–Scuseria–Ernzerhof (HSE) hybrid functional[62] was employed to accurately evaluate the electronic properties. The dynamic stability of the predicted structure was verified by phonon dispersion analysis using the direct supercell method, as implemented in the PHONOPY code.[63]

Experimental procedures TiF_3 was obtained from Alfa Aesar and verified by powder x-ray diffraction (XRD).[16] TiF_3 powder, together with a ruby ball, was loaded into a symmetric diamond-anvil-cell (DAC) with a culet size of 320 μm with no pressure transmitting medium, and the pressure was determined by ruby fluorescence.[64] The sample was first compressed to 20 GPa and then heated to approximately 2000 K using a laser heating system with a diode-pumped CW ytterbium fiber laser (central wavelength of 1080 nm and maximum power of 100 W). Synchrotron XRD patterns were recorded at beamline BL10XU of Spring-8 (Japan) with a wavelength of 0.414 Å, and the refinement was fitted using the GSAS software[65] and EXPGUI interface.[66] *In situ* electrical conductivity measurements, under high pressure and low temperature, were conducted in a DAC equipped with a van der Pauw-type microcircuit.[67]

3. Results and discussion

TiF_3 usually adopts a VF_3-type structure with a space group of *R*–3*c* at ambient pressure,[16,68] in which Ti is surrounded by a tilted octahedron of corner-shared fluorine atoms. The tilting angle of the octahedra decreases with an increase in temperature, leading to a phase transformation from rhombohedral to cubic at 370 K.[20] The cubic structure with the *Pm*-3*m* space group is isostructural in ReO_3, consisting of the TiF_6 octahedra without tilt fluctuations. To determine the high-pressure structure of TiF_3, we performed extensive structural searches at pressures of 20 GPa and 50 GPa. In our structural searches, all the experimental structures of the TiF_3, *R*–3*c*, and *Pm*-3*m* phases were successfully reproduced using the CALYPSO method, validating the reliability of our structure-searching method. In addition to the known experimental structures, an orthorhombic structure with the space group of *Pnma* was successfully observed at 20 GPa.

Enthalpy as a function of pressure for the *Pnma* phase relative to the *R*-3*c* phase is shown in Fig. 1(a). It is apparent that the ambient-pressure phase of *R*–3*c* transforms to the *Pnma* phase at 12 GPa, where the F atoms are in square antiprismatic coordination of the Ti atoms (Fig. 1(b)), which is isostructural to YF_3 at ambient pressure.[69] It is generally accepted that high-pressure phases of lighter elements or compounds in the periodic table are expected to be identical to the ambient structures of the corresponding heavier elements or compounds.[70] At 20 GPa, the largest and average Ti–F bond lengths in the *Pnma* phase are 2.12 Å and 2.05 Å, respectively, while all the bond lengths of Ti–F are equal to 1.93 Å in the *R*–3*c* phase. Furthermore, the coordination number of Ti increases from 6 to 8, weakening individual Ti–F bonds and inducing longer Ti–F bond lengths. Interestingly, compared with the *R*–3*c* phase of TiF_3, in which the A-cation site of the perovskite structure is unoccupied, the newly found high-pressure *Pnma* phase of TiF_3 can be considered a variant perovskite structure with a completely vacant B site. Thus, under certain circumstances, increasing the pressure has demonstrated to be an efficient strategy to tune the vacant coordination sites of cations in perovskites.

We calculated the phonon dispersions of the predicted *Pnma* phase of TiF_3 at 20 GPa (Fig. 1(c)) and observed no imaginary frequencies, indicating that the predicted structure is dynamically stable. Our systematic assessment of energetic and dynamic stabilities suggests that the *Pnma* phase of TiF_3 could be realized experimentally. To verify our theoretical predictions, we performed high-pressure measurements on TiF_3. The synchrotron XRD pattern of TiF_3 was obtained at 20 GPa after laser heating to approximately 2000 K, with Rietveld fitting as shown in Fig. 1(d). The obtained peaks agree well with the predicted orthorhombic *Pnma* structure. The refined lattice parameters of the orthorhombic *Pnma* structure are $a = 5.14$ Å, $b = 6.25$ Å, and $c = 4.38$ Å, which are in excellent agreement with our theoretical results.

After the successful synthesis of the *Pnma* phase in TiF_3, we investigated its bonding characteristics and electronic properties. To determine the nature of the bonding, we examined the electron localization function. A less localized charge distribution is observed in the Ti–F bonds (Fig. 2(a)), indicat-

ing a significant degree of ionicity between the F anions and Ti cations. Furthermore, from Bader charge analysis,[71] the charge values on Ti and F were calculated at 20 GPa. There is a charge transfer of 1.89*e* from Ti to F, comparable to that of typical ionic compounds of NaCl.[72] Moreover, the electronic band structure calculations at the HSE hybrid functional level demonstrated that the *Pnma* phase of TiF_3 is a semiconductor with a band gap of 2.65 eV (Fig. 2(b)). To verify the electrical characteristics of the newly found *Pnma* TiF_3, an *in situ* high pressure electrical conductivity measurement was conducted, based on the van der Pauw-type microcircuit technique.[73] As shown in Fig. 2(c), the electrical resistance monotonically increases with decreasing temperature, confirming the semiconductor characteristics of *Pnma* TiF_3.

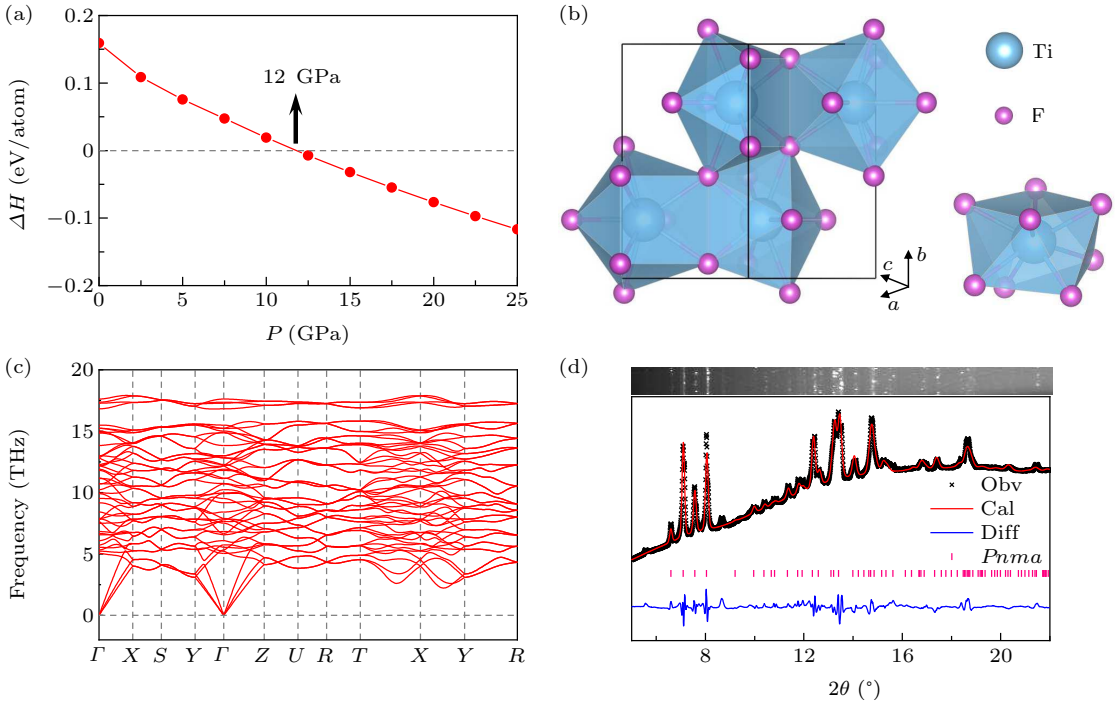


Fig. 1. (a) Enthalpy vs. pressure curves for *Pnma* phase of TiF_3 relative to the *R*–3*c* phase. (b) Crystal structure of the *Pnma* phase formed by TiF_8 square antiprismatic units. The *Pnma* structure contains 16 atoms/cell, wherein Ti atoms occupy the 4*c* (0.13, 0.75, 0.47) positions and the F atoms occupy the 8*d* (0.17, 0.06, 0.65) and 4*c* (0.03, 0.25, 0.13) positions. At 20 GPa, the optimized structural parameters are $a = 5.30$ Å, $b = 6.24$ Å, and $c = 4.40$ Å. (c) Phonon dispersion relations of the *Pnma* phase at 20 GPa. Here, the fractional coordinates of high-symmetry *k* points are given as follows: $\Gamma(0,0,0)$, $X(1/2,0,0)$, $Y(0,1/2,0)$, $Z(0,0,1/2)$, $R(1/2,1/2,1/2)$, $S(1/2,1/2,0)$, $T(0,1/2,1/2)$, $U(1/2,0,1/2)$. (d) Measured powder x-ray diffraction (XRD) pattern of TiF_3 at 20 GPa with Le Bail method (XRD 2D image is given on the top). Vertical ticks correspond to Bragg peaks of the *Pnma* structure (pink). The refined lattice parameters of the orthorhombic *Pnma* structure from the XRD data are $a = 5.14$ Å, $b = 6.25$ Å, and $c = 4.38$ Å. The x-ray wavelength is 0.414 Å.

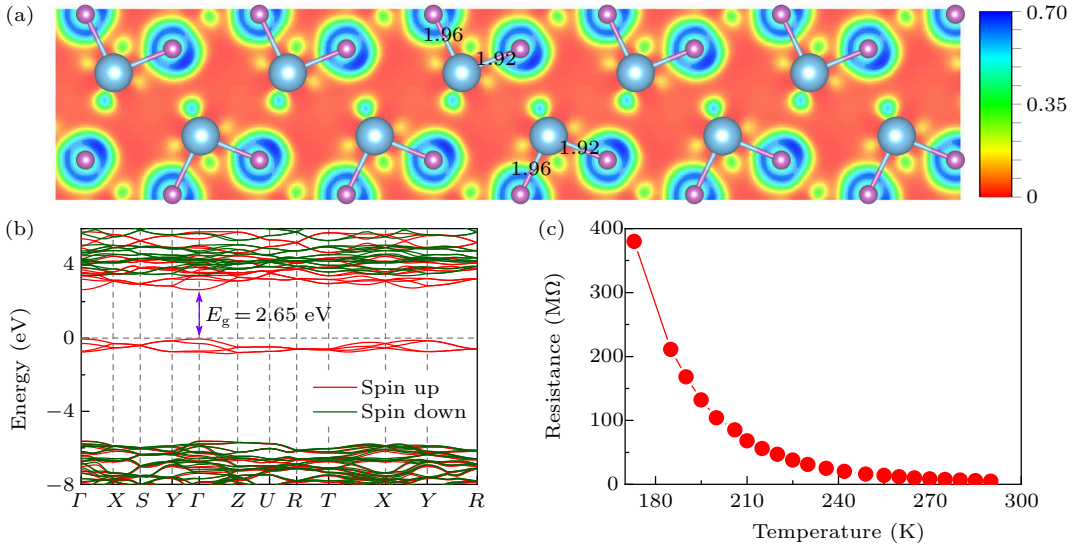


Fig. 2. (a) Calculated ELF of the *Pnma* phase on the (0 1 0) plane at 20 GPa, in which the bond lengths (in units of Å) of the Ti–F bonds are shown. (b) Band structures of the *Pnma* structures at 20 GPa. The red and green colors denote the spin-up and spin-down bands, respectively. The energy of the topmost valence band state is set to 0 eV. Here, the high-symmetry *k* points are the same as those in Fig. 1(c). (c) Experimental resistance–temperature curve of TiF_3 at 20 GPa.

Considering that the *R*–3*c* phase is a prototype structure of transition metal trifluorides under ambient conditions and the discovery of the high-pressure phase of *Pnma* in TiF_3, we deliberated whether this pressure-induced phase transition is a common phenomenon in transition metal trifluorides. Thus, the neighboring metal elements Sc, V, Cr, and Mn were chosen. The enthalpies of the *Pnma* phase as a function of pressure with respect to the *R*-3*c* phase for ScF_3, VF_3, CrF_3, and MnF_3 were calculated and shown in Fig. 3. The phase transition from *R*–3*c* to *Pnma* is a general trend in those metal trifluorides, and the corresponding pressures are calculated to be 5 GPa, 33 GPa, 112 GPa, and 40 GPa for ScF_3, VF_3, CrF_3, and MnF_3, respectively. Therefore, the predicted *Pnma* phase could be a prototype structure widely adopted by transition metal trifluorides at high pressure.

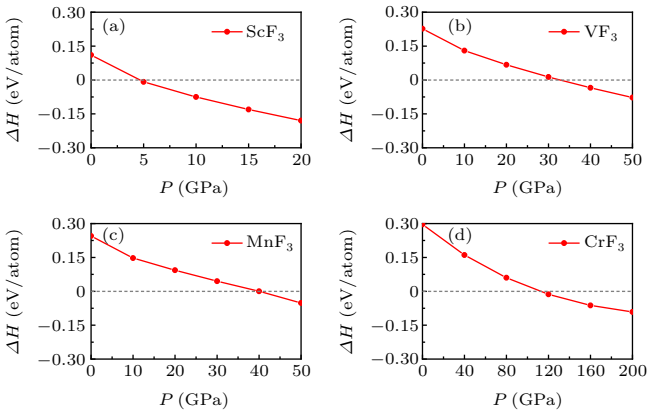


Fig. 3. Calculated enthalpies of *Pnma* phase as functions of pressure with respect to *R*–3*c* phase for ScF_3 (a), VF_3 (b), MnF_3 (c), and CrF_3 (d) systems.

4. Conclusion

In summary, by combining structure-searching methods with first-principle calculations, a pressure-induced *R*-3*c* to *Pnma* phase transition was predicted in TiF_3, which was further confirmed by high-pressure experimental synthesis. The first-principle calculations and electrical measurements demonstrated that the high-pressure *Pnma* phase of TiF_3 exhibits semiconducting characteristics. Further, since the *R*–3*c* phase of TiF_3 is a prototype structure for transition metal trifluorides at ambient pressure, it was shown that the pressure-induced phase transition from *R*-3*c* to *Pnma* is a general trend in transition metal trifluorides.

Acknowledgments

Project supported by the National Natural Science Foundation of China (Grant Nos. 12034009, 91961204, and 11974134). Part of the calculation was performed in the high-performance computing center of Jilin University and the School of Physics and Electronic Engineering of Jiangsu Normal University.

References

[1] Corrales-Salazar A, Brierley R T, Littlewood P B and Guzmán-Verri G G 2017 *Phys. Rev. Mater.* **1** 053601
[2] HandunkandaS U, Curry E B, Voronov V and Hancock J N 2019 *J. Phys.: Condens. Matter* **32** 035403
[3] Han F, Chen J, Hu L, Ren Y, Rong Y, Pan Z, Deng J and Xing X 2016 *J. Am. Ceram. Soc.* **99** 2886
[4] Wang L, Yuan P F, Wang F, Sun Q, Liang E J, Jia Y and Guo Z X 2014 *Phys. Lett. A* **378** 2906
[5] Arai H, Okada S, Sakurai Y and Yamaki J 1997 *J. Power Sources* **68** 716
[6] Nishijima M, Gocheva I D, Okada S, Doi T, Yamaki J and Nishida T 2009 *J. Power Sources* **190** 558
[7] Wang J, Li F, Yang B, Liu X and Zhao M 2017 *J. Mater. Chem. A* **5** 21486
[8] Wang P, Kang X D and Cheng H M 2005 *Appl. Phys. Lett.* **87** 071911
[9] Wang P, Kang X D and Cheng H M 2005 *ChemPhysChem* **6** 2488
[10] Hou X, Hu R, Zhang T, Kou H, Li J and Xue X 2013 *Int. J. Hydrog. Energy* **38** 12904
[11] Guo Y H, Yu X B, Gao L, Xia G L, Guo Z P and Liu H K 2010 *Energy Environ. Sci.* **3** 465
[12] Li Y, Zhang Y and Chen L 2021 *Front. Chem.* **9** 693302
[13] Mondal P, Opalka D, Poluyanov L V and Domcke W 2012 *J. Chem. Phys.* **136** 084308
[14] Perebeinos V and Vogt T 2004 *Phys. Rev. B* **69** 115102
[15] Greve B K, Martin K L, Lee P L, Chupas P J, Chapman K W and Wilkinson A P 2010 *J. Am. Chem. Soc.* **132** 15496
[16] Siegel S 1956 *Acta Crystallogr.* **9** 684
[17] Daniel P, Bulou A, Leblanc M, Rousseau M and Nouet J 1990 *Mater. Res. Bull.* **25** 413
[18] Hepworth M A, Jack K H, Peacock R D and Westland G J 1957 *Acta Crystallogr.* **10** 63
[19] Hepworth M A and Jack K H 1957 *Acta Crystallogr.* **10** 345
[20] Kennedy B J and Vogt T 2002 *Mater. Res. Bull.* **37** 77
[21] Jiang S, Fang Y, Li R, Xiao H, Crowley J, Wang C, WhiteT J, Goddard III W A, Wang Z, Baikie T and Fang J 2016 *Angew. Chem. Int. Ed.* **128** 6650
[22] Li Q, Zhang L, Chen Z and Quan Z 2019 *J. Mater. Chem. A* **7** 16089
[23] Szafranski M and Katrusiak A 2016 *J. Phys. Chem. Lett.* **7** 3458
[24] Zhang R, Cai W, Bi T, Zarifi N, Terpstra T, Zhang C, Verdeny Z V, Zurek E and Deemyad S 2017 *J. Phys. Chem. Lett.* **8** 3457
[25] Wang Y, LüX, Yang W, Wen T, Yang L, Ren X, WangL, Lin Z and Zhao Y 2015 *J. Am. Chem. Soc.* **137** 11144
[26] Kong L, Liu G, Gong J, Hu Q, Schaller R D, Dera P, Zhang D, Liu Z, Yang W, Zhu K, Tang Y, Wang C, WeiS H, Xu T and Mao H K 2016 *Proc. Natl. Acad. Sci. USA* **113** 8910
[27] Guennou M, Bouvier P, Toulemonde P, Darie C, Goujon C, Bordet P, Hanfland M and Kreisel J 2014 *Phys. Rev. Lett.* **112** 075501
[28] Lee J H, Jaffe A, Lin Y, Karunadasa H I and Neaton J B 2020 *ACS Energy Lett.* **5** 2174
[29] Duan D, Liu Y, Tian F, Li D, Huang X, Zhao Z, Yu H, Liu B, Tian W and Cui T 2014 *Sci. Rep.* **4** 6968
[30] Drozdov A P, Eremets M I, Troyan I A, Ksenofontov V and Shylin S I 2015 *Nature* **525** 73
[31] Drozdov A P, Kong P P, Minkov V S, Besedin S P, Kuzovnikov M A, Mozaffari S, Balicas L, Balakirev F F, Graf D E, Prakapenka V B, Greenberg E, Knyazev D A, Tkacz M and Eremets M I 2019 *Nature* **569** 528
[32] Somayazulu M, Ahart M, Mishra A K, Geballe Z M, BaldiniM, Meng Y, Struzhkin V V and Hemley R J 2019 *Rev. Lett.* **122** 027001
[33] Snider E, Dasenbrock-Gammon N, McBride R, Debessai M, Vindana H, Vencatasamy K, Lawler K V, Salamat A and Dias R P 2020 *Nature* **586** 373
[34] Li T, Jiang S, Sivadas N, Wang Z, Xu Y, Weber D, Goldberger J E, Watanabe K, Taniguchi T, Fennie C J, Mak K F and Shan J 2019 *Nat. Mater.* **18** 1303
[35] Jiang S Q, Yang X, Huang X L, Huang Y P, Li X and Cui T 2020 *Chin. Phys. Lett.* **37** 016102
[36] Zhao X Y, Huang J H, Zhuo Z Y, Xue Y Z, Ding K, Dou X M, Liu J and Sun B Q 2020 *Chin. Phys. Lett.* **37** 044204
[37] Wang W D, Li A, Xu G H, Wang P, Liu Y G and Wang L P 2020 *Chin. Phys. Lett.* **37** 058101

[38] Wang J, Zhou Q, Guo S, Huang Y, Huang X, Wang L, Li F and Cui T 2020 *Chin. Phys. Lett.* **37** 066201
[39] Lei L, Tang Q Q, Zhang F, Liu S, Wu B B and Zhou C Y 2020 *Chin. Phys. Lett.* **37** 068101
[40] Hong F, Yang L, Shan P, Yang P, Liu Z, Sun J, Yin Y, Yu X, Cheng J and Zhao Z 2020 *Chin. Phys. Lett.* **37** 107401
[41] Sowa H and Ahsbahs H 1998 *Acta Crystallogr., Sect. B:Struct. Sci.* **54** 578
[42] Jørgensen J E, Marshall W G and Smith R I 2004 *Acta Crystallogr. Sect. B: Struct. Sci.* **60** 669
[43] Zhu F, Lai X, Wu X, Li Y and Qin S 2014 *Acta Crystallogr. Sect. B: Struct. Sci.* **70** 801
[44] Wang Y, Lv J, Zhu L and Ma Y 2010 *Phys. Rev. B* **82** 094116
[45] Wang Y, Lv J, Zhu L and Ma Y 2012 *Comput. Phys. Commun.* **183** 2063
[46] Gao B, Gao P, Lu S, Lv J, Wang Y and Ma Y 2019 *Sci. Bull.* **64** 301
[47] Zhang J, Lv J, Li H, Feng X, Lu C, Redfern S A, Liu H, Chen C and Ma Y 2018 *Phys. Rev. Lett.* **121** 255703
[48] Sun Y, Lv J, Xie Y, Liu H and Ma Y 2019 *Phys. Rev. Lett.* **123** 097001
[49] Xu M, Zhan G, Liu S, Zhang D, Zhong X, Qu Z, Li Y, Du A, Zhang H and Wang Y 2019 *Phys. Rev. B* **100** 235435
[50] Xu M, Huang C, Li Y, Liu S, Zhong X, Jena P, Kan E and Wang Y 2020 *Phys. Rev. Lett.* **124** 067602
[51] Zhang M G, Yan H Y, Zhang G T and Wang H 2012 *Chin. Phys. B* **21** 076103
[52] Zhang G T, Bai T T, Zhao Y R and Lu C 2013 *Chin. Phys. B* **22** 116104
[53] Chu B H, Zhao Y and Wang D H 2021 *Chin. Phys. B* **30** 046101
[54] Guo Y L, Wei J H, Liu X, Ke X Z and Jiao Z Y 2021 *Chin. Phys. B* **30** 016101
[55] Shi X H, Liu B, Yao Z and Liu B B 2020 *Chin. Phys. Lett.* **37** 047101
[56] Lv R Y, Yang X G, Yang D W, Niu C Y and Zhao C X 2021 *Chin. Phys. Lett.* **38** 076101
[57] Liu Y X, Wang C, Han S, Chen X, Sun H R and Liu X B 2021 *Chin. Phys. Lett.* **38** 036201
[58] Kohn W and Sham L J 1965 *Phys. Rev.* **140** A1133
[59] Kresse G and Hafner J 1993 *Phys. Rev. B* **47** 558
[60] Blöchl P E 1994 *Phys. Rev. B* **50** 17953
[61] Perdew J P, Burke K and Ernzerhof M 1996 *Phys. Rev. Lett.* **77** 3865
[62] Heyd J, Scuseria G E and Ernzerhof M 2003 *J. Chem. Phys.* **118** 8207
[63] Parlinski K, Li Z Q and Kawazoe Y 1997 *Phys. Rev. Lett.* **78** 4063
[64] Mao H K, Bell P M, Shaner J W and Steinberg D J 1978 *J. Appl. Phys.* **49** 3276
[65] Larson A C and Von Dreele R B 2000 *General StructureAnalysis System (GSAS)*, Los Alamos National Laboratory Report LAUR 86–748
[66] Toby B H 2001 *J Appl. Crystallogr.* **34** 210
[67] Li M, Gao C X, Ma Y Z, He C Y, Hao A M, Zhang D M, Li Y C, Liu J and Jun W D 2007 *Chin. Phys. Lett.* **24** 1010
[68] Jack K H and Gutmann V 1951 *Acta Crystallogr.* **4** 246
[69] Zalkin A and Templeton D H 1953 *J. Am. Chem. Soc.* **75** 2453
[70] Hemley R J 1998 *Ultrahigh Pressure Mineralogy-Physics and Chemistry of the Earth's Deep Interior* (Washington, DC: Mineralogical Society of America) chapter 9, p. 283
[71] Tang W, Sanville E and Henkelman G 2009 *J. Phys.: Condens. Matter* **21** 084204
[72] Chen X and Ma Y 2012 *Europhys. Lett.* **100** 26005
[73] Luong D H, Phan T L, Ghimire G, Duong D L and Lee Y H 2019 *APL Mater.* **7** 081102